Stochastic models for transport in a fluidized bed

Dehling, H.G; Hoffmann, A.C; Stuut, H.W.

Published in:
Siam Journal on Applied Mathematics

DOI:
10.1137/S0036139996306316

SIAM J. APPL. MATH.
Vol. 60, No. 1, pp. 337–358

STOCHASTIC MODELS FOR TRANSPORT IN A FLUIDIZED BED*

H. G. DEHLING†, A. C. HOFFMANN‡, AND H. W. STUUT†

Abstract. In this paper we study stochastic models for the transport of particles in a fluidized bed reactor and compute the associated residence time distribution (RTD). Our main model is basically a diffusion process in $[0, A]$ with reflecting/absorbing boundary conditions, modified by allowing jumps to the origin as a result of transport of particles in the wake of rising fluidization bubbles. We study discrete time birth-death Markov chains as approximations to our diffusion model. For these we can compute the particle distribution inside the reactor as well as the RTD by simple and fast matrix calculations. It turns out that discretization of the reactor into a moderate number of segments already gives excellent numerical approximations to the continuous model. From the forward equation for the particle distribution in the discrete model we obtain in the diffusion limit a partial differential equation for the particle density $p(t, x)$

$$\frac{\partial}{\partial t}p(t,x) = \frac{1}{2}\frac{\partial^2}{\partial x^2}[D(x)p(t,x)] - \frac{\partial}{\partial x}[v(x)p(t,x)] - \lambda(x)p(t,x)$$

with boundary conditions $p(t, 1) = 0$ and

$$\frac{1}{2}\frac{\partial}{\partial x}[D(x)p(t,x)]_{|x=0} - v(0)p(t,0) - \int_0^1 \lambda(x)p(t,x)dx = 0.$$

Here $v(x)$ and $D(x)$ are the velocity and the diffusion coefficients and $\lambda(x)$ gives the rate of jumps to the origin.

We also study a model allowing a discrete probability of jumps to the origin from the distributor plate, thus incorporating the experimentally observed fact that a fixed percentage of particles gets caught in the wake of gas bubbles during their formation at the bottom of the reactor. It turns out that this effect contributes to an extra term to the boundary condition at $x = 0$.

Finally, we model the particle flow in the wakes of rising fluidization bubbles and derive $\lambda(x)$ as well as $v(x)$. We compare our results with experimental data.

Key words. Markov processes, diffusion approximation, stochastic modeling, transport phenomena, residence time distribution, chemical reactors, fluidized beds, partial differential equations

AMS subject classifications. Primary, 60J25; Secondary, 60J70, 92E20

PII. S0036139996306316

1. Introduction.

In this paper we study the transport of particles in a certain type of chemical reactor, with special emphasis on computing residence time distributions. The reactor we will consider is a fluidized bed reactor. A fluidized bed is obtained by forcing gas upward through a bed of powder. This is done through a distributor plate permeable to the fluidizing gas but not to the particles. If the gas velocity is high enough, the bed will be supported in the gas stream, the particles entering a more or less floating state. The bed will then exhibit liquid-like behavior. If the gas velocity is increased further, fluidization bubbles will start to form and rise through the bed much as in a boiling liquid. A further feature of the bed considered here is that it is "continuous," meaning that particles are added to (and removed from) the bed continuously. The process is shown schematically in Figure 1.

*Received by the editors July 8, 1996; accepted for publication (in revised form) December 22, 1998; published electronically December 21, 1999.
http://www.siam.org/journals/siap/60-1/30631.html

†Department of Mathematics, University of Groningen, Blauwborgje 3, 9747 AC Groningen, The Netherlands (dehling@math.rug.nl).

‡Department of Chemical Engineering, University of Groningen, Nijenborgh 4, 9747 AG Groningen, The Netherlands (a.c.hoffmann@chem.rug.nl).

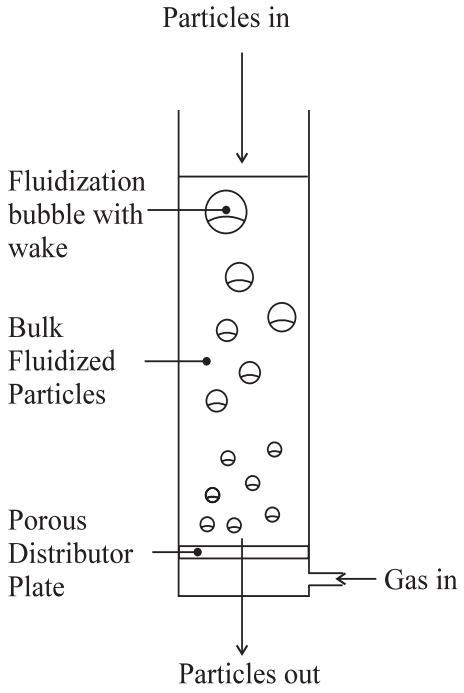

FIG. 1. *Fluidized bed reactor. Fluidizing air is introduced through the porous support plate. The fluidization bubbles increase in size with height in the bed due to coalescence, as does the bubble wake fraction and, therefore, the material transport in the wake phase.*

A number of studies in the scientific literature are dedicated to predicting the particle residence time distribution (RTD) in such continuous fluidized beds. In most of this work attempts have been made to formulate semiempirical models using the traditional tools of RTD theory. Klose and Herschel [10] and Pudel, Strümke, and Sündermann [15] used series of ideal mixers. They fitted the number of mixers to match predictions to experimental results. Another modeling approach has been based on plug flow with superimposed dispersion, where the dispersion coefficient was adjusted to fit experimental data [13], [20], [18].

However, a discrepancy between the model predictions and the actual behavior of continuous fluidized beds remained when using these simple approaches. Whittmann et al. [22] tried series of ideal mixers with reverse flow, and Heertjes, de Nie, and Verloop [7] tried a model incorporating combinations of ideal mixers in series and in parallel. Krishnaiah, Pydisetty, and Varma [11] proposed a model with a combination of a mixed section with a stagnant one and short circuiting.

A few studies have attempted to take the actual physical phenomena occurring in a continuous fluidized bed into consideration. Berrutti, Liden, and Scott [1] proposed a model based on a series of compartments in the fluidized bed each with gross solid circulation. Morris, Gubbins, and Watkins [14] presented a model based on the proposed existence of a velocity profile in the vertically moving fluidized solids, similar to the profile in a viscous fluid flowing in a pipe. Haines, King, and Woodburn [5] used the plug flow with axial dispersion approach, but they augmented their dispersion coefficient (which they assumed was caused mostly by the random collisional movement of individual particles) with a term accounting for the extra dispersion caused

by rising fluidization bubbles.

Rowe and Partridge [17] first proposed physical processes governing the vertical particle transport processes in batch fluidized beds. These are (see also Figure 1)

- transport upward in bubble wakes and deposition on top of the bed,
- transport down in the bulk due to the removal of material low in the bed in bubble wakes ("circulation"), and
- dispersion due to the disturbance of the bulk material by fluidization bubbles.

Hoffmann and Paarhuis [8] showed by means of a computer simulation that these processes could account also for the RTD of particles in continuous fluidized beds. In this article a mathematical model based on these principles—and starting with a stochastic model for the particle motion in the bed—is formulated, solved, and compared with experimental results. We believe that stochastic models for the motion of an individual particle should be the basis for an analysis of the evolution of the particle density over time. Such models are easily made—at least for a discrete approximation—and have a stronger intuitive appeal than traditional macroscopic models. The macroscopic description in terms of PDEs with boundary conditions can, of course, be derived from the stochastic model.

Our mathematical analysis is based on a Markovian model for the motion of individual particles through the reactor. Denoting the vertical distance of the particle from the top of the reactor at time t by X_t, we model the motion by a stochastic process (X_t). We first study a discrete model, obtained by dividing the reactor into N horizontal cells of equal width and modeling the particle's location at integer times only. The cells are numbered from top to bottom, with an extra cell with index $N+1$ denoting the lower exit of the reactor. Particles that have entered state $N+1$ cannot return to the interior of the reactor. The dynamics of our process is described by a Markov chain $(X_n)_{n\geq 0}$ with state space $\{1, 2, \ldots, N+1\}$ and an absorbing boundary at $N+1$. Our Markov chain is basically a birth-death process, modified to allow for instant jumps to the first cell—thus modeling the possibility that a particle gets caught in the wake of a rising gas bubble (see Figure 2).

We show that this simple model gives rise to RTDs that capture the main features of empirically observed RTDs in fluidized beds. We show that the long tails of the RTD function are a consequence of the fact that the second-largest eigenvalue of our Markov transition matrix is very close to 1.

In reality, the transport process occurs in continuous space and time, and thus we should also study continuous models. We introduce such models as limits of discrete Markov chains, obtained by letting space and time discretizations converge to zero in an appropriate way. The limit process is an ordinary diffusion process with reflecting/absorbing boundary conditions, modified to allow for instant jumps to the origin. We derive a PDE for the particle density $p(t, x)$ in the continuous model which then also provides the RTD function via $F(t) = 1 - \int_0^1 p(t, x)dx$. We show numerically that the particle density and the RTD function of the continuous model can be well approximated by the corresponding functions in the discrete model, provided the discretization is fine enough—for all practical purposes, $N = 50$ cells turned out to be sufficient.

In the last section we take a model for the particle flow in the wakes of rising gas bubbles as basis for modeling the parameters of the continuous jump-diffusion model. For several parameter settings we compare the model RTD with experimental values. It turns out that our theoretically obtained RTD functions capture the main features of the experimental RTDs quite well.

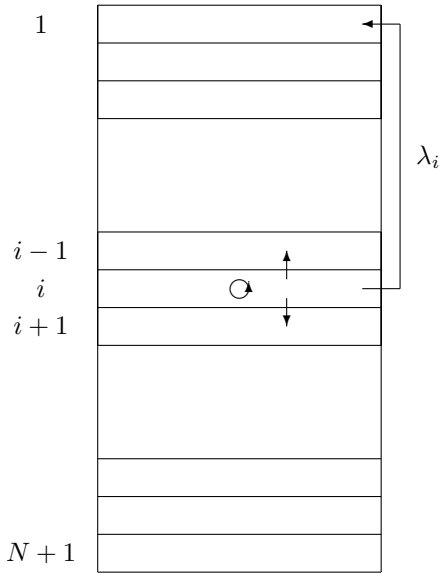

FIG. 2. *Discrete Markov model for transport in a fluidized bed. The reactor is vertically partitioned into N cells of equal width, with cell $N+1$ symbolizing the exterior of the reactor. The possible transitions are that a particle can move one cell down, stay in the same cell, move one cell up, or move to the top of the reactor.*

2. Discrete Markov model. In this section we study discrete mathematical models for particle transport in a fluidized bed. We discretize space by subdividing the interior of the reactor into N horizontal cells of equal width, labeled $i = 1, 2, \ldots, N$, and identifying the lower exit of the reactor with the index $i = N + 1$. Time is discretized by considering the particle position at integer times only. We denote the index of the cell that the particle visits at time n by X_n. We model the dynamics of the process by assuming that $(X_n)_{n\geq 0}$ forms a Markov chain. This Markov chain is fully specified once we know

1. the probability vector $p(0) = (p(0,1), \ldots, p(0,N+1))$ of the particle's initial position, where $p(0,i) = P(X_0 = i)$, and
2. the transition matrix $P = (p_{ij})_{1\leq i,j\leq N+1}$, where p_{ij} gives the conditional probability that the particle is in cell j at time $n+1$, given it was in cell i at time n, i.e., $p_{ij} = P(X_{n+1} = j | X_n = i)$.

Probabilities of arbitrary events concerning $(X_n)_{n\geq 0}$ can then be computed. For example, the probability that the particle starts at time $n = 0$ in cell i_0, then visits cells $i_1, \ldots, i_{n-1}$, and finally at time n ends up in cell i_n is given by $p(0,i_0)p_{i_0 i_1} \ldots p_{i_{n-1} i_n}$.

DEFINITION 1. *We define the probability function of X_n by*

$$p(n,i) = P(X_n = i).$$

The corresponding probability vector is denoted by $p(n)$.

By conditioning on the particle's position at time $n-1$, we obtain the recursion formula

$$p(n,j) = \sum_{i=1}^{N+1} p(n-1,i)p_{ij}, \tag{1}$$

which in matrix notation becomes $p(n) = p(n-1)P$. Iterating this identity, we obtain the explicit formula $p(n) = p(0)P^n$ for the probability distribution of the particle's location at time n. In what follows we always assume that the particle starts in the first cell; hence $p(0) = (1, 0, \ldots, 0)$. Then $p(n)$ is simply the first row of the nth power of the transition matrix.

From a macroscopic point of view, the probability vector $p(n)$ gives the distribution of particles over the cells if at time $n = 0$ a large number of particles was placed in the first cell. In such a setup, (1) can be interpreted as a mass-balance equation.

An important characteristic of a reactor is its RTD. We define the residence time of a particle as the time the particle spends inside the reactor. Since a particle that has left the reactor cannot return to the inside, the residence time equals the first exit time $T = \inf_{n\geq 0}\{X_n = N+1\}$. The residence time distribution is the distribution of T and can be described either by its cumulative distribution function $F(n) = P(T \leq n)$ or by its probability function $f(n) = P(T = n)$. As $T \leq n$ if and only if $X_n = N+1$, we have the simple identity

$$F(n) = P(T \leq n) = p(n, N+1),$$

and $f(n) = p(n, N+1) - p(n-1, N+1)$, for $n = 1, 2, \ldots$.

Our starting point is a conventional birth-death model, where a particle positioned at i can move one step ahead with probability β_i, one step back with probability δ_i, or stay in the present location with probability $\alpha_i = 1 - \beta_i - \delta_i$. We add to this the possibility of a complete return to the origin, whose probability is denoted by λ_i, thus modeling the chance that the particle gets caught in the wake of a gas bubble (see Figure 2). In this way we obtain the following transition probabilities for the interior of the reactor, i.e., for $2 \leq i \leq N$:

$$\begin{aligned} p_{i,1} &= \lambda_i, \\ p_{i,i-1} &= \delta_i(1-\lambda_i), \\ p_{i,i} &= \alpha_i(1-\lambda_i), \\ p_{i,i+1} &= \beta_i(1-\lambda_i) \end{aligned} \tag{2}$$

(for $i = 2$ the probability $p_{2,1}$ is obtained by adding the first two probabilities, resulting in $\lambda_2 + \delta_2(1-\lambda_2)$). Regarding the boundaries, we assume reflection at the origin and absorption at $i = N+1$, i.e.,

$$\begin{aligned} p_{1,1} &= 1 - \beta_1(1-\lambda_1), \\ p_{1,2} &= \beta_1(1-\lambda_1), \\ p_{N+1,N+1} &= 1. \end{aligned} \tag{3}$$

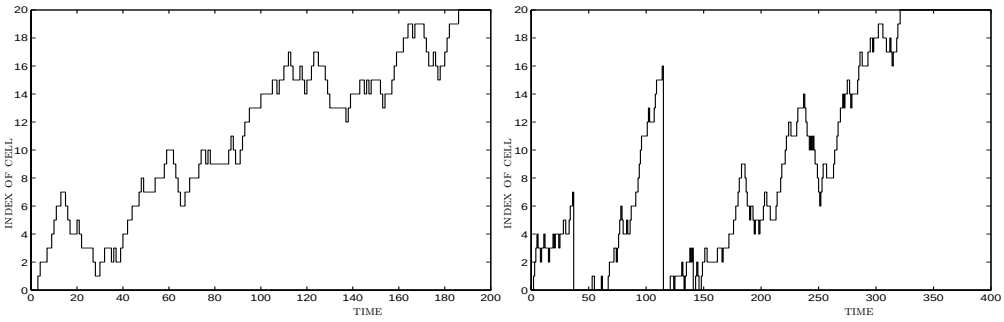

FIG. 3. *Simulation of a path in the discrete Markov model for two different parameter settings.* $N = 20$ *cells,* $\delta_i = 0.2, \alpha_i = 0.5, \beta_i = 0.3$ *in both cases, and return probabilities* $\lambda_i \equiv 0$ *(left) or* $\lambda_i \equiv 0.01$ *(right). The horizontal axis denotes time, the vertical axis the index of the cell.*

The last cell ($i = N+1$) is identified with the exterior of the reactor from where there is no return to the reactor. The full transition matrix for this model is then

$$\begin{pmatrix} 1-\beta_1(1-\lambda_1) & \beta_1(1-\lambda_1) & 0 & 0 & \dots & 0 & 0 \\ \lambda_2+\delta_2(1-\lambda_2) & \alpha_2(1-\lambda_2) & \beta_2(1-\lambda_2) & 0 & \dots & 0 & 0 \\ \lambda_3 & \delta_3(1-\lambda_3) & \alpha_3(1-\lambda_3) & \beta_3(1-\lambda_3) & \dots & 0 & 0 \\ \lambda_4 & 0 & \delta_4(1-\lambda_4) & \alpha_4(1-\lambda_4) & \dots & 0 & 0 \\ \vdots & \vdots & \vdots & \vdots & \ddots & \vdots & \vdots \\ \lambda_N & 0 & 0 & 0 & \dots & \alpha_N(1-\lambda_N) & \beta_N(1-\lambda_N) \\ 0 & 0 & 0 & 0 & \dots & 0 & 1 \end{pmatrix}.$$

Thus if the corresponding Markov chain does not return to the first cell, then it is an ordinary birth-death process with transition probabilities δ_i, α_i, β_i and reflecting/absorbing boundary conditions. The return probability is, in general, state dependent. However, in the special case where all λ_i's are constant and equal to λ, say, the return times are independent of the state of the process. The return times then form a Bernoulli process with intensity λ (i.e., simply a coin-tossing process with probability of heads equal to λ). The complete transport process is then decomposed into two independent parts, namely, the return process and a sequence of birth-death processes between return times.

In Figure 3 we have simulated two runs of the transport process for two different choices of the parameters. In both cases we have $N = 20$ cells, and $\delta_i \equiv 0.2$, $\alpha_i \equiv 0.5$, and $\beta_i = 0.3$. This results in a mean velocity inside the reactor of $v = 0.1$ and a dispersion of $D = 0.49$. The return probabilities differ. In the left simulation they are equal to 0, and in the right simulation they are constant equal to 0.01. The choice of $\lambda_i \equiv 0.01$ in the right simulation is somewhat, but not completely, arbitrary. We want to present an example of our Markov process that shows how the possibility of a jump back to the origin influences the evolution of the particle density and the RTD. In order to show the main effects, one has to choose the parameters in such a way that there is a reasonable but not dominating chance for a full return. In our example the speed is .1 cells per unit of time; hence a rough calculation shows that it takes on average $T = 200$ time units to pass through the reactor yielding an average of about two full returns.

In principle, one can obtain the particle distribution at any time as well as the RTD function by Monte Carlo simulations. However, this requires an extremely large number of simulations and is therefore computationally slow. For our discrete models,

exact computations that make use of the recursion formula (1) are much faster. Due to the lower tridiagonal structure of the transition matrix, (1) becomes

$$p(n+1,i) = (1-\lambda_{i-1})\beta_{i-1}p(n,i-1) + (1-\lambda_i)\alpha_i p(n,i) + (1-\lambda_{i+1})\delta_{i+1}p(n,i+1) \tag{4}$$

for $2 \le i \le N$, together with the boundary conditions

$$p(n+1,1) = \sum_{i=1}^{N} \lambda_i p(n,i) + \delta_2(1-\lambda_2)p(n,2) + (1-\lambda_1)(1-\beta_1)p(n,1), \tag{5}$$

$$p(n+1,N+1) = \beta_N(1-\lambda_N)p(n,N) + p(n,N+1). \tag{6}$$

These equations are discrete analogues of the Fokker–Planck equations.

In Figure 4 we have plotted the probability distribution of the particle's location after $n = 25$, 50, and 100 steps for the parameter settings corresponding to the simulations in Figure 3. In the top row the distribution has in the interior and for small n the characteristic Gaussian shape with center roughly at nv and standard deviation $\sqrt{nD}$, which for larger values of n gets distorted by the absorbing boundary. The shape is completely different in the middle row due to the returns to the first cell. The height of the last column in these plots gives the probability that the particle has left the reactor by time n, and that is just the value of the cumulative RTD function at time n. In Figure 4 we have plotted the complete cumulative RTD functions for the two parameter settings. The most striking difference between the two RTDs lies in the tail of the distribution. For the model with a positive return probability the tail is extremely heavy, a characteristic which is also encountered in experimental results.

Understanding the tail behavior of the RTD requires a study of the probability vector $p(n) = p(0)P^n$ for large values of n through the eigenvalues and eigenvectors of P. The transition matrix P has a unique invariant distribution, namely, $\rho = (0,\dots,0,1)$. Up to normalization, ρ is the unique left eigenvector with eigenvalue 1. By the Perron–Frobenius theorem, all other eigenvalues are of modulus less than 1. Moreover, $p(0)P^n \to \rho$ regardless of the initial distribution. We are interested in the difference $p(n)-\rho$, and this turns out to be governed by the second-largest eigenvalue of P and the corresponding eigenvector.

THEOREM 1. *Suppose that P has a full set of left eigenvectors $u_0 = \rho$, $u_1,\dots,u_N$ corresponding to eigenvalues $\mu_0 = 1, \mu_1, \mu_2, \dots, \mu_N$ in decreasing order of magnitude. If $|\mu_2| < |\mu_1|$, there exist constants k_1 and k_2 such that*

$$1 - F(n) = k_1\mu_1^n + O(\mu_2^n),$$
$$p(n,i) = k_2\mu_1^n u_1(i) + O(\mu_2^n)$$

for $1 \le i \le N$.

Proof. We can write $p(0)$ as a linear combination of the eigenvectors $p(0) = a_0\rho + a_1u_1 + \cdots + a_Nu_N$. From this we get

$$p(n) = p(0)P^n = a_0\rho + \mu_1^n a_1u_1 + \mu_2^n a_2u_2 + \cdots + \mu_N^n a_N u_N = \rho + \mu_1^n a_1u_1 + O(\mu_2^n),$$

as $p(0)P^n \to \rho$ requires $a_0 = 1$. The last coordinate in the above vector identity implies

$$1 - F(n) = \rho(N+1) - p(n,N+1) = -a_1u_1(N+1)\mu_1^n + O(\mu_2^n) = k_1\mu_1^n + O(\mu_2^n).$$

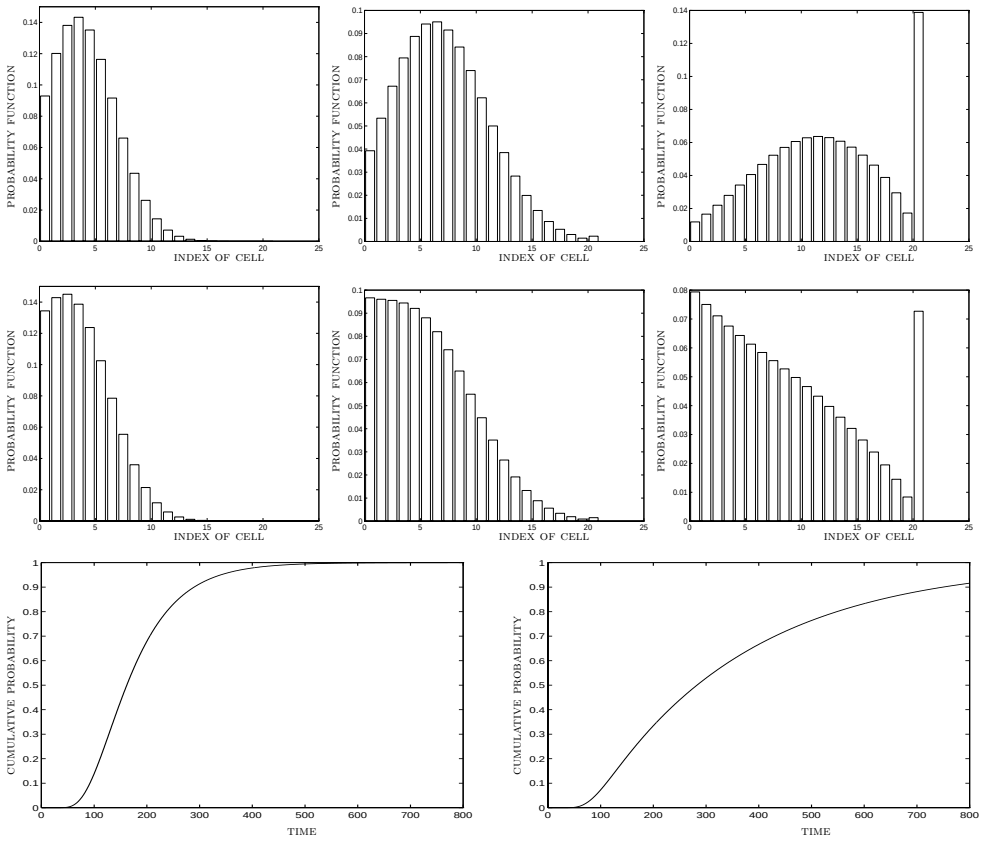

FIG. 4. *Evolution of particle density and cumulative RTD function in the discrete Markov model for two parameter settings.* $N = 20$ *cells,* $\delta_i = 0.2$, $\beta_i = 0.3$ *in both cases and return probability* $\lambda_i \equiv 0$ *(top row and bottom left) or* $\lambda_i \equiv 0.01$*(middle row and bottom right). In the top and middle row, the density is shown at time points* $n = 25, 50, 100$ *(from left to right), with horizontal axis showing the index of the cell and vertical axis showing the occupation probability. In the bottom row the RTD curve is shown, with axes showing time and cumulative probability.*

For $1 \leq i \leq N$ we have $\rho(i) = 0$ and hence $p(n, i) = a_1 \mu_1^n u_1(i)$. □

We see that the probability distribution inside the reactor has a shape determined by u_1. Moreover, $F(n)$ converges to 1 exponentially fast at a rate $\log \mu_1$. Hence a fat tail of the RTD corresponds to μ_1 being close to 1. We can indeed verify this for the second of the examples studied above. Here $\mu_1 = 0.9966$, accounting for the slow convergence of $F(n)$ to 1. In Figure 5, top, we have plotted approximations $\{k_1 \mu_1^n u_1(i), 1 \leq i \leq N\}$ for $n = 100$ and $n = 200$ together with the exact probability functions. For $n = 200$ the difference is no longer visible. On the bottom we have plotted the exact cumulative RTD function $F(n)$ together with $1 - k_2 \mu_1^n$.

The numerical computations in this section have been carried out by implementation of the recursion formula (1) in MATLAB. In this way, the computation of, e.g., the particle distribution at time $n = 1000$ for the case of $N = 50$ cells takes less than one second on an HP workstation.

3. Diffusion limits. In this section we will study the transport model of the previous section in the limit as the discretization steps converge to 0. Throughout the

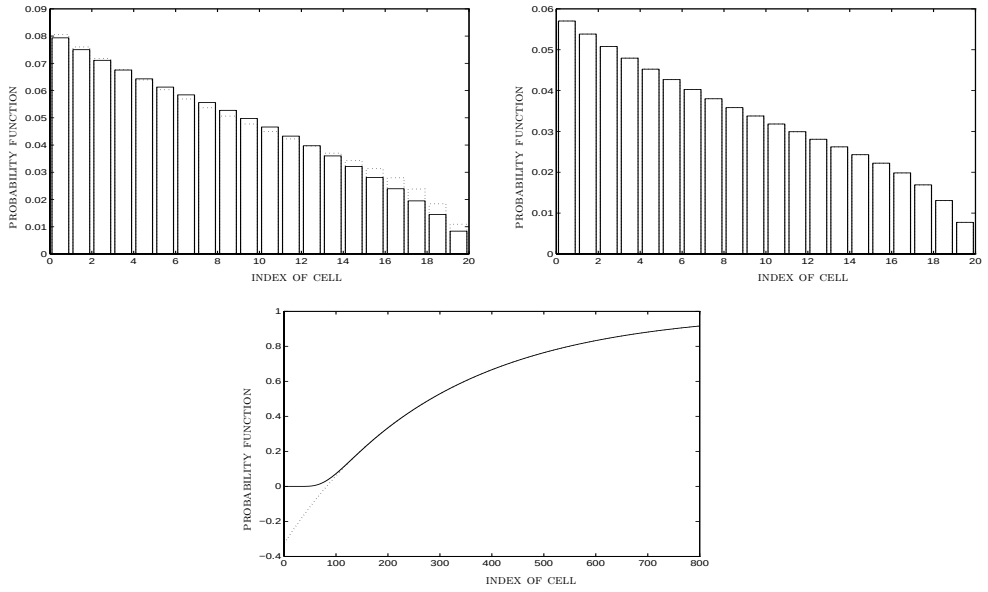

FIG. 5. *Density profiles in the interior of the reactor at large times.* $n = 100$ *(top left) or* $n = 200$ *(top right), and cumulative RTD function (bottom), with parameter values* $N = 20$, $\delta_i \equiv 0.2$, $\beta_i \equiv 0.3$, *and* $\lambda_i \equiv 0.01$. *The dotted lines show the approximations derived from Theorem* 1*—note that at* $n = 200$ *the approximation is almost perfect.*

remainder of the paper we shall assume that we are dealing with a cylindrical reactor of height 1. By x we denote the vertical distance from the top of the reactor—i.e., $x = 0$ corresponds to the top and $x = 1$ to the bottom. We divide the reactor into N horizontal segments of height $\Delta = 1/N$ each. The x-coordinate of a particle in cell i is then in $((i-1)\Delta, i\Delta]$, $i = 1, 2, \ldots, N+1$. Time is discretized into intervals of length ϵ, and we will model the particle's position at times $n\epsilon$, $n = 0, 1, 2, \ldots$.

In order to obtain a limit as $\epsilon, \Delta \to 0$, we have to let the probabilities β_i, δ_i, and λ_i depend on ϵ and Δ in a suitable way. To do so, we will first express β_i and δ_i in terms of physically meaningful quantities, namely, the particle velocity and the diffusion coefficient. Let $v(x)$ and $D(x)$ be functions on $[0, 1]$ denoting velocity and diffusion at x, respectively. We define

$$\beta_i = \frac{\epsilon}{2\Delta^2} D(i\Delta) + \frac{\epsilon}{2\Delta} v(i\Delta),$$
$$\delta_i = \frac{\epsilon}{2\Delta^2} D(i\Delta) - \frac{\epsilon}{2\Delta} v(i\Delta),$$

and $\alpha_i = 1 - \delta_i - \beta_i$. A particle located at time $n\epsilon$ in the cell $((i-1)\Delta, i\Delta]$ will, until time $(n+1)\epsilon$, either stay in the same cell, move to one of the neighboring cells $((i-2)\Delta, (i-1)\Delta]$ and $(i\Delta, (i+1)\Delta]$, or return to the first cell. Conditioned on the last possibility not occurring, the probabilities for the first three transitions are α_i, δ_i, and β_i, respectively. With these choices of probabilities, the mean displacement per step becomes $\epsilon v(i\Delta)$, which corresponds to a mean velocity of $v(i\Delta)$. The mean square displacement per step is given by $\Delta^2(\beta_i + \delta_i) = \epsilon D(i\Delta)$, resulting in a mean square displacement per unit of time of $D(i\Delta)$. We define, moreover, $D_0 = \sup_{0 \le x \le 1} D(x)$

and let ϵ depend on Δ via

$$\epsilon = \frac{\Delta^2}{2D_0}.$$

Under the assumption that v and D are continuous functions with values in $(0, \infty)$, we get that the probabilities α_i, β_i, and δ_i are positive for small enough Δ.

Modeling the possibility of a complete return to the origin, we assume that particles return at a rate $\lambda(x)$, i.e., that a particle located at x has a probability $\epsilon\lambda(x)$ to be picked up in the wake of a gas bubble during a time period of length ϵ. In total we get the following probabilities in the interior, i.e., for $i = 2, \ldots, N$:

$$\begin{aligned}
p_{i,i-1} &= \left[\frac{\epsilon}{2\Delta^2} D(i\Delta) - \frac{\epsilon}{2\Delta} v(i\Delta)\right](1 - \epsilon\lambda(i\Delta)),\\
p_{i,i} &= \left[1 - \frac{\epsilon}{\Delta^2} D(i\Delta)\right](1 - \epsilon\lambda(i\Delta)),\\
p_{i,i+1} &= \left[\frac{\epsilon}{2\Delta^2} D(i\Delta) + \frac{\epsilon}{2\Delta} v(i\Delta)\right](1 - \epsilon\lambda(i\Delta)),\\
p_{i,1} &= \epsilon\lambda(i\Delta).
\end{aligned}$$

For the boundaries, we again assume reflection at the origin and absorption in the last cell, i.e.,

$$\begin{aligned}
p_{1,1} &= \left[1 - \left\{\frac{\epsilon}{2\Delta^2} D(\Delta) + \frac{\epsilon}{2\Delta} v(\Delta)\right\}\right](1 - \epsilon\lambda(\Delta)),\\
p_{1,2} &= \left[\frac{\epsilon}{2\Delta^2} D(\Delta) + \frac{\epsilon}{2\Delta} v(\Delta)\right](1 - \epsilon\lambda(\Delta)),\\
p_{N+1,N+1} &= 1.
\end{aligned}$$

We assume that a particle is initially in the first cell and denote by $\tilde{X}_n^\Delta$ its location (i.e., number of corresponding cell) after n transitions. Then the distance from the top at time t is given by

$$X_t^\Delta = \Delta \cdot \tilde{X}_{[t/\epsilon]}^\Delta,$$

approximately. It is heuristically obvious that as $\Delta \to 0$, the process X_t^Δ converges to a limit process (X_t), though we do not have a rigorous mathematical proof. For ordinary birth-death processes, i.e., without jumps to the origin, this convergence is well known (see Bhattacharya and Waymire [2]). In our case, the limit process is basically a diffusion process with reflecting/absorbing boundary, with the additional possibility of a jump back to the origin. In general, the jump intensity is location-dependent and therefore the jump process depends on the diffusion part. In the case of a homogeneous return rate $\lambda(x) \equiv \lambda$, a simple description of (X_t) is possible. Now this process decomposes into two independent parts; a Poisson process of jumps with intensity λ and a sequence of diffusion processes between the jumps.

Let $\tilde{p}_\Delta(n, i)$ denote the probability that a particle is in cell i after n transitions, i.e., $\tilde{p}_\Delta(n, i) = P(\tilde{X}_n^\Delta = i)$. Assuming that the distribution is uniformly spread over the cell, we have at time t the particle density

$$p_\Delta(t, x) = \frac{1}{\Delta} \tilde{p}_\Delta([t/\epsilon], [x/\Delta]).$$

As $\Delta \to 0$, we expect $p_\Delta(t, x)$ to converge to the particle density $p(t, x)$ of the limit process X_t. The probability that the particle has left the reactor by time t is given by

$$F_\Delta(t) := \tilde{p}_\Delta([t/\epsilon], N + 1),$$

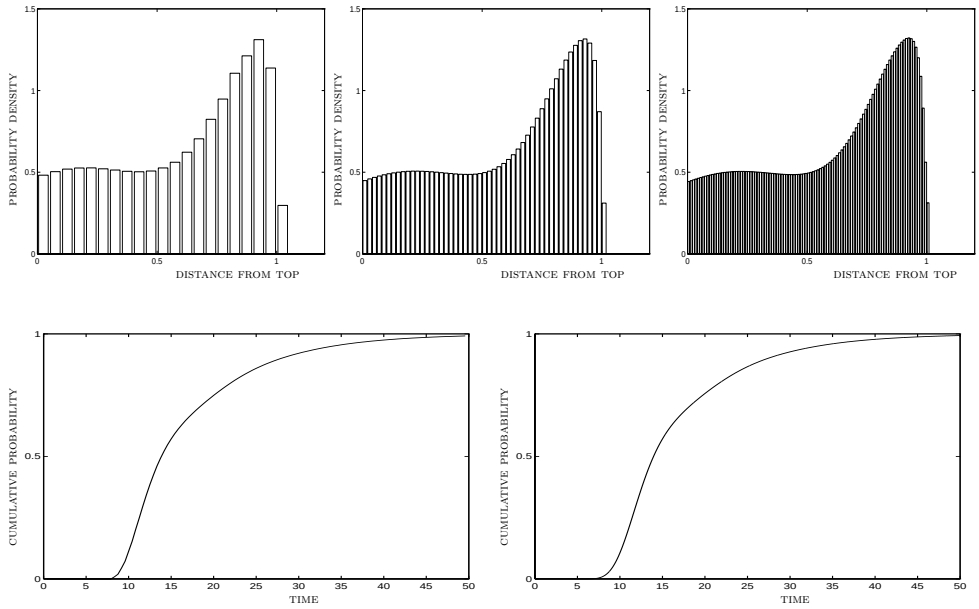

FIG. 6. *Particle density at $t = 12$ (top row) and cumulative RTD function (bottom row) for different discretizations of the continuous model. Parameters are $D(x) \equiv 0.003$, $v(x) \equiv 0.08$, $\lambda(x) \equiv 0.05$ and cell widths $\Delta = 0.05$ (top and bottom left), $\Delta = .02$ (top middle), and $\Delta = .01$ (top and bottom right).*

and we expect this to converge to the cumulative RTD of (X_t). In Figure 6 we have plotted the particle density in the interior of the reactor for the parameter setting $D = .003$, $v = .08$, $\lambda = .05$ at time $t = 12$ at three different discretizations, namely, for $N = 20, 50, 100$. The height of the last column gives the probability that the particle has reached the boundary, i.e., $F_\Delta(t)$. Indeed, these plots show the fast convergence both of the particle density in the interior and of $F_\Delta(t)$. This is also confirmed by the plot of the full cumulative RTD function.

From (4) we obtain a recursion formula for $p_\Delta(n\epsilon, i\Delta)$, namely,

$$
\begin{aligned}
&p_\Delta((n+1)\epsilon, i\Delta) \\
&= \left\{ \frac{\epsilon}{2\Delta^2} D((i-1)\Delta) + \frac{\epsilon}{2\Delta} v((i-1)\Delta) \right\} [1 - \epsilon\lambda((i-1)\Delta)] p_\Delta(n\epsilon, (i-1)\Delta) \\
&\quad + \left\{ 1 - \frac{\epsilon}{\Delta^2} D(i\Delta) \right\} [1 - \epsilon\lambda(i\Delta)] p_\Delta(n\epsilon, i\Delta) \\
&\quad + \left\{ \frac{\epsilon}{2\Delta^2} D((i+1)\Delta) - \frac{\epsilon}{2\Delta} v((i+1)\Delta) \right\} [1 - \epsilon\lambda((i+1)\Delta)] p_\Delta(n\epsilon, (i+1)\Delta)
\end{aligned} \tag{7}
$$

for $i = 1, 2, \ldots, N-2$. In the appendix we shall show that as $\Delta, \epsilon \to 0$, this difference equation goes over into the following PDE for the limit density

$$
\frac{\partial}{\partial t} p(t,x) = \frac{1}{2} \frac{\partial^2}{\partial x^2} (D(x) p(t,x)) - \frac{\partial}{\partial x} (v(x) p(t,x)) - \lambda(x) p(t,x). \tag{8}
$$

The boundary conditions in the limit become

$$
\int_0^1 \lambda(x) p(t,x) dx + \frac{1}{2} \frac{\partial}{\partial x} (D(x) p(t,x))_{|x=0} - v(0) p(t,0) = 0
$$

at the entrance to the cylinder and $p(t,1) = 0$ at the exit. We have not been able to solve this PDE analytically, although a series expansion seems feasible for the case of constant velocity, diffusion, and return rate. The computations for the discretized model can be viewed as numerical approximations to the solution of (8).

The cumulative RTD function gives the probability that a particle has left the reactor by time t and can be computed from the particle density $p(t,x)$ by

$$F(t) = 1 - \int_0^1 p(t,x)dx.$$

Again the cumulative RTD function for the discretized model can be viewed as numerical approximation to $F(t)$.

Experiments have shown that, in addition to the continuous removal of particles from the interior of the reactor, there is a discrete return probability at the distributor plate due to the formation of gas bubbles there. A fraction Λ of all the particles that get to the distributor plate is picked up in the wake of a gas bubble and deposited at the top of the reactor. Only the remaining fraction $1 - \Lambda$ leaves the reactor immediately. In our model we incorporate this effect by changing the transition probabilities from the Nth cell to

$$\begin{aligned} p_{N,1} &= \Lambda, \\ p_{N,N+1} &= 1 - \Lambda. \end{aligned}$$

In the appendix we shall show that the particle density for the limit is again the solution to the same PDE (8), but now with the following boundary condition at $x = 0$:

$$\int_0^1 \lambda(x)p(t,x)dx - \frac{\Lambda}{1-\Lambda}\frac{\partial}{\partial t}\int_0^1 p(t,x)dx + \frac{1}{2}\frac{\partial}{\partial x}(D(x)p(t,x))_{|x=0} - v(0)p(t,0) = 0.$$

We shall compute the RTD function for this model in the next section in connection with a choice of the parameters motivated by physical considerations.

4. Comparison with experiments. In a physical reactor, the average downward speed $v(x)$ and the removal rate $\lambda(x)$ are not independent parameters—removal of mass from the reactor below x increases the speed above x. Both $v(x)$ and $\lambda(x)$, as well as Λ, can be calculated from the flow of mass in the wake of rising fluidization bubbles. Here we first attempt to model this flow.

As mentioned in the introduction, particles are picked up in the wakes of rising fluidization bubbles and carried to the top of the bed, where they are deposited. It is known that the total region enclosing the bubble with its wake is approximately spherical. The fraction of this sphere taken up by wake material is often called the "wake fraction," f_W; this increases with the size of the fluidization bubble. As fluidization bubbles rise, they grow through coalescence. The total flow of empty bubble void remains approximately constant over the bed height, which means that the total flow of material in the wake increases. Material is therefore caught up in bubble wake

1. upon formation of the bubbles at the distributor plate, and
2. as the flow in the bubble wake grows with height in the bed.

The former is in the mathematical model represented by a discrete probability Λ. The latter is represented by $\lambda(x)$, the probability intensity of a Poisson process modeling the pickup of a particle in bubble wakes as it travels downward through the bed.

It should be noted that most researchers also operate with material exchange between the bubble wake and its surroundings as the fluidization bubble rises. Hoffmann, Janssen, and Prince [9], however, have shown it likely that this interchange in the main is driven by a difference in bulk density between the bubble wake and the surroundings; such a difference is not present if the particles in the bed are uniform.

The two parameters Λ and $\lambda(x)$ can be quantified on basis of empirical relations in the literature. The wake angle has been found to increase with increasing bubble size. An empirical relationship is

$$\theta_W = 2.8 - 2.8\exp(-60D_B) \tag{9}$$

(see [8]), giving after some trigonometric calculations the wake fraction, f_W. As mentioned, the bubble size increases with height in the bed due to coalescence of bubbles. Geldart [4] gives an empirical relation for the bubble size as a function of height in the bed:

$$D_B = \frac{1.3}{g^{0.2}}\left(\frac{U-U_{mf}}{1000}\right)^{0.4}\left(\frac{1}{1-f_W}\right)^{0.33} + 2.05h(U-U_{mf})^{0.94}. \tag{10}$$

The first term in (10) gives the bubble size upon formation at the distributor plate, and the second accounts for the growth due to coalescence. A complication is that the first term contains the wake fraction, f_W, that again depends on D_B. The initial bubble diameter, therefore, has to be found iteratively.

The total flow of empty bubble volume is normally assumed to be given by the so-called two-phase theory. This theory says that any gas flow in excess of the flow required just to fluidize the powder (superficial velocity U_{mf}) flows through the bed in the form of bubbles:

$$Q_B = A(U-U_{mf}), \tag{11}$$

where A is the cross-sectional area of the bed. The number of bubbles passing a cross section at any height in the bed per second, N_B, can then be calculated:

$$N_B = \frac{A(U-U_{mf})}{\frac{\pi}{6}D_B^3(1-f_W)}. \tag{12}$$

The total rate of transport of material in the bubble wakes at any height in the bed is then

$$Q_W = N_B\frac{\pi}{6}D_B^3 f_W. \tag{13}$$

A particle introduced in the top of the bed will move downward in the bulk toward the distributor plate as long as it is not caught in a bubble wake and deposited on top of the bed again. The downward velocity of a particle in the bulk consists of two contributions:

1. a contribution due to the inflow and outflow from the bed, and
2. a contribution arising from the removal of material from the bed below the particle by bubble wakes.

The first contribution is easily calculated as a superficial velocity v_0 equal to the volumetric inflow per unit cross-sectional area, (Q_{in}/A). The second contribution decreases as the particle moves down the bed. The total rate of removal of material

TABLE 1
List of cases for which the mathematical model was evaluated.

Case	Q_{in}/A (m/s)	$U - U_{mf}$ (m/s)	h (m)	Λ
1	$4.00 * 10^{-3}$	$1.50 * 10^{-2}$	0.10	$9.27 * 10^{-2}$
2	$4.00 * 10^{-3}$	$3.00 * 10^{-2}$	0.10	$3.10 * 10^{-1}$
3	$2.00 * 10^{-3}$	$3.00 * 10^{-2}$	0.10	$4.73 * 10^{-1}$
4	$5.19 * 10^{-5}$	$5.40 * 10^{-3}$	0.0977	$2.36 * 10^{-1}$
5	$8.88 * 10^{-5}$	$2.58 * 10^{-3}$	.0977	$3.03 * 10^{-2}$
6	$5.26 * 10^{-5}$	$4.44 * 10^{-2}$	.107	$9.71 * 10^{-1}$
7	$6.78 * 10^{-5}$	$6.90 * 10^{-3}$	.0933	$2.95 * 10^{-1}$
8	$4.29 * 10^{-4}$	$1.55 * 10^{-2}$	0.23	$3.54 * 10^{-1}$
9	$4.29 * 10^{-4}$	$2.35 * 10^{-2}$	0.23	$5.74 * 10^{-1}$

below the position x of the particle is equal to Q_W/A; Q_W was calculated in (13). The total value of the velocity of the particle is therefore

$$v(x) = v_0 + \frac{Q_W(x)}{A}.$$

In order to compute the removal rate $\lambda(x)$, we consider a segment between height x and $x + \Delta x$ in the container. In a time interval of length Δt, there is a flow $\Delta t Q_W(x)$ into the segment and an outflow $\Delta t Q_W(x + \Delta x)$. As the total volume of the segment is $\Delta x \cdot A$, we get that the fraction of removed material equals

$$\frac{\Delta t[Q_W(x + \Delta x) - Q_W(x)]}{\Delta x A},$$

which, as $\Delta x \to 0$, yields a return rate

$$\lambda(x) = \frac{d}{dx}\frac{Q_W}{A}.$$

At the distributor plate, the fluidization bubbles with their wake are formed. There is here a finite discrete probability that a particle gets caught in the wake. Just above the distributor plate, the flow is $Q_W(1)/A + v_0$, below it is v_0, and hence a fraction

$$\Lambda = \frac{Q_W(1)/A}{Q_W(1)/A + v_0}$$

gets removed. This completes the evaluation of the model parameters.

Table 1 shows the cases for which the mathematical model was evaluated.

The first three cases are hypothetical, chosen to test the qualitative variation of the predicted RTD curves with the operational parameters. The last six are cases for which experimental data are available in the literature: Cases 4–7 in la Riviére et al. [12] and Cases 8–9 in Morris, Gubbins, and Watkins [14].

Werther [21] and others have shown that the two-phase theory generally overestimates the gas flow in the bubble phase. It is possible from the plots constructed by Werther to assess roughly the severity of this overestimation for the experimental cases listed in Table 1. In accordance with this, the values of $U - U_{mf}$ were reduced by a factor of 2/3 in Cases 4, 5, 6, and 7 and with a factor of 3/4 in Cases 8 and 9.

Figure 7 shows the results of the simulations of Cases 1, 2, and 3. The figure shows that the model predicts influences of the operating variables qualitatively in line with

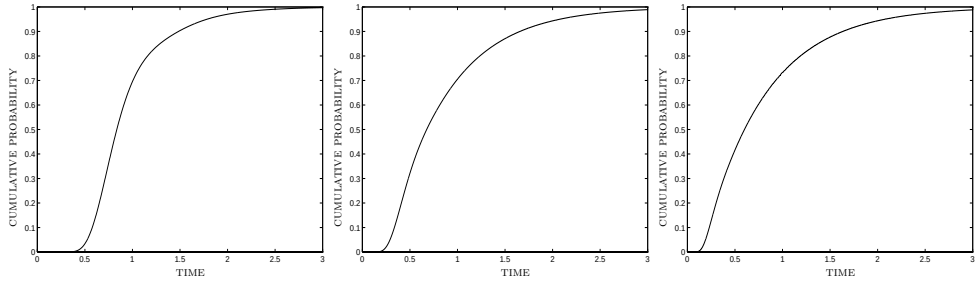

FIG. 7. *Cumulative RTD function for Cases* 1–3 *in Table* 1, *showing the effects of the throughflow* (Q_{in}/A) *and bubbling intensity* ($U - U_{mf}$).

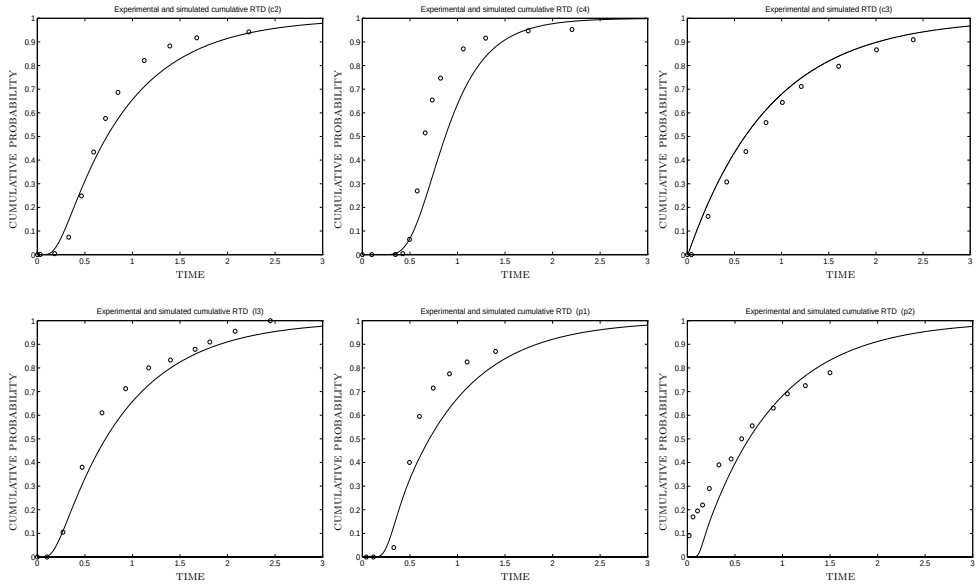

FIG. 8. *Cumulative RTD function for Cases* 4–9 *in Table* 1. *Points are experimentally determined data from the literature, and curves are the predictions of the model.*

the experimental evidence in the literature. An increase in the excess superficial gas velocity $U - U_{mf}$ causes an increase in the mixing for equal solid throughflow, while an increase in solid throughflow for equal excess gas flow causes a tendency toward plug-flow (diffusion-free flow of particles at constant speed and without the possibility of returns to the top of the reactor). For plug-flow, the RTD curve would be a Heaviside function $F(t) = 1_{[1,\infty)}(t)$, and for ideal mixing it would be an exponential function $F(t) = 1 - e^{-t}$ $(t > 0)$. Indeed one can see in Figure 7 a continuous transition from near plug-flow to near ideal mixing as the bubbling intensity becomes more significant relative to the solids throughflow.

In Figure 8 model predictions are compared with the experimentally determined RTDs for Cases 4–9. Cases 4–7 are taken from [12]. These measurements were performed in beds of an internal diameter of 8.8 cm using colored (Cases 4–6) and slightly larger (Case 7) tracer particles. Cases 8–9 are taken from [14], who used a

colored tracer in a bed of 23 cm diameter. All these cases fall within the range of "bubbling fluidization," to which the model is applicable. The model describes neither bubble-free fluidization (fine particles fluidized at low gas velocities) nor turbulent fluidization (fluidization at very high gas velocities). The most interesting results are obtained for relatively low "internal flow ratios" (Hartholt [6]), defined as the upward flow of particles in the bubble wakes divided by the downward flow due to the throughput.

The model predictions agree quite well with the experimental points. Both prediction and experiment show an almost well mixed system in Cases 6 and 9, where the value of $U - U_{mf}$ is relatively high. Also in the cases where the system tends to exhibit more plug-flow-like behavior (Cases 4, 5, 7, and 8) the agreement is good and, in particular, the points of initial rise of the F-curve are well predicted by the model. This shows that the envisaged mixing conditions can account for the behavior seen experimentally. It also shows that a good fit is obtained, even though the quantification of the parameters is performed on basis of the literature, and the model, therefore, in this sense does not contain any adjustable parameter.

Nevertheless, a consistent discrepancy between model predictions and experiment can be seen in Figure 8. The experimental points generally rise more sharply than the model predictions and in one or two cases it appears that the experimental data show a longer tail than do the model predictions.

Figure 9 shows a so-called intensity curve, the intensity being defined as

$$I(t) = \frac{dF(t)/dt}{1 - F(t)}. \tag{14}$$

Under conditions of steady flow, Verloop, de Nie, and Heertjes [19] showed that continuous fluidized beds exhibit a characteristic shape for $I(t)$, the graph showing a maximum for a value of the dimensionless time between 0 and 1. The present model also shows such a local maximum for Cases 8 and 9 and a weaker one for Case 5, while in the other cases a maximum is not visible on the plots. It can also be seen in Figure 9 that the intensity approaches a constant value at larger values of the dimensionless residence time. This is in line with our earlier findings about the dominance of a single eigenvalue in the tail of the RTD curve.

5. Conclusions. In this paper we propose a birth-death process with jumps as a model for the transport of particles in a fluidized bed reactor. We show numerically that the RTD for this model captures the main features of experimentally observed RTD functions. Moreover, we study mathematical aspects of our model. We prove that the tail behavior of the RTD function can be understood from the second-largest eigenvalue of the transition matrix. We investigate the diffusion limit of our discrete process and find the Fokker–Planck equation for the particle density.

We believe that the discrete time stochastic process modeling approach for transport of particles can be useful also in other types of reactors, and thus is of relevance beyond the specific reactor and the specific model that have been studied here. Our approach has several attractive features:

- The models are easily formulated, based on physical ideas about the motion of a single particle.
- The models are computationally easy to handle, especially with a matrix-oriented package like MATLAB.
- The discrete models provide a very good approximation to the physically more reasonable continuous models. As continuous models require much more

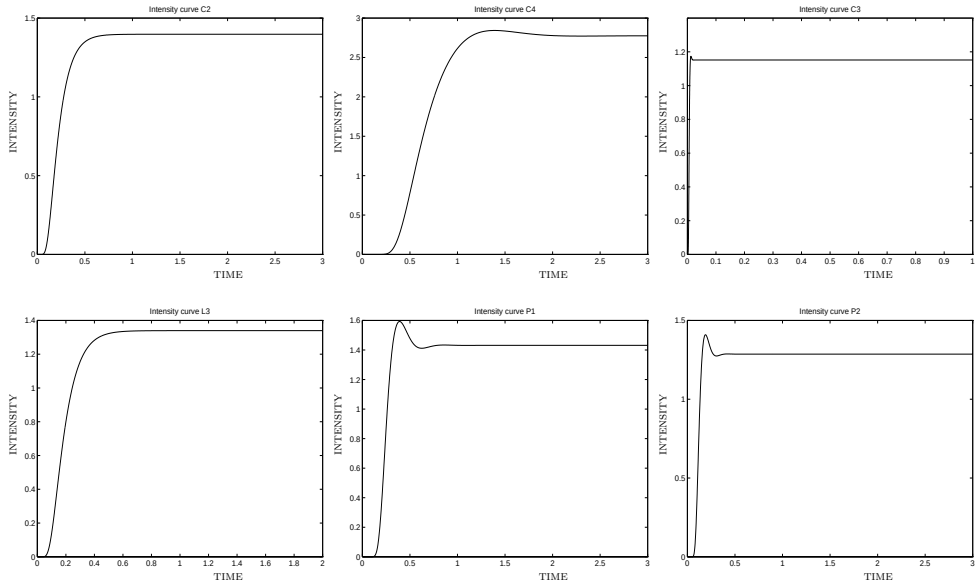

FIG. 9. *Intensity curves for Cases* 4–9 *in Table* 1. *The curves for Cases* 6, 8, *and* 9 *exhibit a local maximum. Such a maximum was found experimentally by Verloop, de Nie, and Heertjes* [19] *to be characteristic of the particle RTD in continuous fluidized beds.*

sophistication in both formulation and analysis, this makes discrete models attractive.

- If desired, traditional PDEs for particle densities can be obtained as limits of discrete Fokker–Planck equations by letting the discretization steps converge to 0.

The present paper provides only a first step toward a rigorous mathematical analysis of our particle transport process, at the same time raising many problems for future research. One problem is to study existence and uniqueness of solutions to the continuous Fokker–Planck equation (8) and to establish rigorously convergence of $p_\Delta(t,x)$ to a solution of (8). Another interesting problem is to study eigenvalues and eigenfunctions of (8) in order to understand the tail behavior of the RTD function. Of special interest is the dependence of the second-largest eigenvalue on the model parameters, and then especially on the return rate $\lambda(x)$. A challenging statistical problem is to develop techniques for estimation of model parameters from empirical RTD curves. Also extensions of the present model, e.g., by taking into account the finite speed of upward transport in the wakes, should be a fruitful area of research.

6. Appendix. We will show here that the difference equation (7) for the approximate density of the particle inside the reactor converges in the diffusion limit to the PDE (8) for the density $p(t,x)$. We obtain for $i = 2, \dots, N-1$

$$
\begin{aligned}
&p_\Delta((n+1)\epsilon, i\Delta) \\
&= \left\{ \frac{\epsilon}{2\Delta^2} D((i-1)\Delta) + \frac{\epsilon}{2\Delta} v((i-1)\Delta) \right\} [1 - \epsilon\lambda((i-1)\Delta)] p_\Delta(n\epsilon, (i-1)\Delta) \\
&+ \left\{ 1 - \frac{\epsilon}{\Delta^2} D(i\Delta) \right\} [1 - \epsilon\lambda(i\Delta)] p_\Delta(n\epsilon, i\Delta)
\end{aligned}
$$

$$
\begin{aligned}
&+\left\{\frac{\epsilon}{2\Delta^2}D((i+1)\Delta)-\frac{\epsilon}{2\Delta}v((i+1)\Delta)\right\}[1-\epsilon\lambda((i+1)\Delta)]p_\Delta(n\epsilon,(i+1)\Delta)\\
&=\left\{\frac{\epsilon}{2\Delta^2}D((i-1)\Delta)+\frac{\epsilon}{2\Delta}v((i-1)\Delta)\right\}\\
&\times\ [p_\Delta(n\epsilon,(i-1)\Delta)-\epsilon\lambda((i-1)\Delta)p_\Delta(n\epsilon,(i-1)\Delta]\\
&+\left\{1-\frac{\epsilon}{\Delta^2}D(i\Delta)\right\}[p_\Delta(n\epsilon,i\Delta)-\epsilon\lambda(i\Delta)p_\Delta(n\epsilon,i\Delta)]\\
&+\left\{\frac{\epsilon}{2\Delta^2}D((i+1)\Delta)-\frac{\epsilon}{2\Delta}v((i+1)\Delta)\right\}[p_\Delta(n\epsilon,i\Delta)-\epsilon\lambda((i+1)\Delta)p_\Delta(n\epsilon,(i+1)\Delta)]\\
&=\left\{\frac{\epsilon}{2\Delta^2}D((i-1)\Delta)+\frac{\epsilon}{2\Delta}v((i-1)\Delta)\right\}p_\Delta(n\epsilon,(i-1)\Delta)\\
&+\left\{1-\frac{\epsilon}{\Delta^2}D(i\Delta)\right\}p_\Delta(n\epsilon,i\Delta)\\
&+\left\{\frac{\epsilon}{2\Delta^2}D((i+1)\Delta)-\frac{\epsilon}{2\Delta}v((i+1)\Delta)\right\}p_\Delta(n\epsilon,i\Delta)\\
&-\epsilon\lambda(i\Delta)p_\Delta(n\epsilon,i\Delta)+o(\epsilon).
\end{aligned}
$$

Subtracting $p_\Delta(n\epsilon,i\Delta)$ from both sides and dividing by ϵ, we get

$$
\begin{aligned}
&\frac{p_\Delta((n+1)\epsilon,i\Delta)-p_\Delta(n\epsilon,i\Delta)}{\epsilon}\\
&\quad=\frac{1}{2\Delta^2}\{D((i-1)\Delta)p_\Delta(n\epsilon,(i-1)\Delta)-2D(i\Delta)p_\Delta(n\epsilon,i\Delta)\\
&\qquad+D((i+1)\Delta)p_\Delta(n\epsilon,(i+1)\Delta)\}\\
&\qquad+\frac{1}{\Delta}\{v((i-1)\Delta)p_\Delta(n\epsilon,(i-1)\Delta)-v((i+1)\Delta)p_\Delta(n\epsilon,(i+1)\Delta)\}\\
&\qquad-\lambda(i\Delta)p_\Delta(n\epsilon,i\Delta)+o(1).
\end{aligned}
$$

As $\Delta,\epsilon\to 0$ and $n\epsilon\approx t$, $i\Delta\approx x$, this difference equation approaches the PDE (8). At the entrance to the reactor we obtain the boundary condition

$$
\begin{aligned}
p_\Delta((n+1)\epsilon,\Delta)&=\epsilon\sum_{i=1}^{N}\lambda(i\Delta)p_\Delta(n\epsilon,i\Delta)\\
&\quad+(1-\epsilon\lambda(\Delta))\left(1-\frac{\epsilon}{2\Delta^2}D(\Delta)-\frac{\epsilon}{2\Delta}v(\Delta)\right)p_\Delta(n\epsilon,\Delta)\\
&\quad+(1-\epsilon\lambda(2\Delta))\left(\frac{\epsilon}{2\Delta^2}D(2\Delta)-\frac{\epsilon}{2\Delta}v(2\Delta)\right)p_\Delta(n\epsilon,2\Delta)\\
&=\epsilon\sum_{i=1}^{N}\lambda(i\Delta)p_\Delta(n\epsilon,i\Delta)+\left(1-\frac{\epsilon}{2\Delta^2}D(\Delta)-\frac{\epsilon}{2\Delta}v(\Delta)\right)p_\Delta(n\epsilon,\Delta)\\
&\quad+\left(\frac{\epsilon}{2\Delta^2}D(2\Delta)-\frac{\epsilon}{2\Delta}v(2\Delta)\right)p_\Delta(n\epsilon,2\Delta)+O(\epsilon).
\end{aligned}
$$

Subtracting $p_\Delta(n\epsilon,\Delta)$ from both sides and multiplying by Δ/ϵ we get

$$
\begin{aligned}
&\Delta\frac{p_\Delta((n+1)\epsilon,\Delta)-p_\Delta(n\epsilon,\Delta)}{\epsilon}\\
&\quad=\Delta\sum_{i=1}^{N}\lambda(i\Delta)p_\Delta(n\epsilon,i\Delta)+\frac{1}{2\Delta}\{D(2\Delta)p_\Delta(n\epsilon,2\Delta)-D(\Delta)p_\Delta(n\epsilon,\Delta)\}\\
&\qquad-\left\{\frac{1}{2}v(\Delta)p_\Delta(n\epsilon,\Delta)+\frac{1}{2}v(2\Delta)p_\Delta(n\epsilon,\Delta)\right\}+O(\Delta).
\end{aligned}
\tag{15}
$$

As $\Delta \to 0$, the left-hand side converges to zero, and we get in the limit the boundary condition

$$\int_0^1 \lambda(x)p(t,x)dx + \frac{1}{2}\frac{\partial}{\partial x}(D(x)p(t,x))_{|x=0} - v(0)p(t,0) = 0.$$

The boundary condition in the absorbing boundary $x = 1$ can be obtained from similar considerations. One obtains

$$\lim_{x \nearrow 1} p(t,x) = 0.$$

For the model including the discrete return probability at the distributor plate, we obtain the same PDE for the interior of the reactor and the same boundary condition at the exit. In the derivation of the boundary condition at $x = 0$ we have to replace the right-hand side of (15) by

$$\Delta \sum_{i=1}^{N} \lambda(i\Delta)p_\Delta(n\epsilon, i\Delta) + \frac{1}{2\Delta}\{D(2\Delta)p_\Delta(n\epsilon, 2\Delta) - D(\Delta)p_\Delta(n\epsilon,\Delta)\}$$
$$- \left\{\frac{1}{2}v(\Delta)p_\Delta(n\epsilon,\Delta) + \frac{1}{2}v(2\Delta)p_\Delta(n\epsilon,\Delta)\right\} + \frac{\Delta}{\epsilon}\Lambda p_\Delta(n\epsilon, N\Delta) + O(\Delta).$$

Regarding the last summand we note that

$$F_\Delta((n+1)\epsilon) - F_\Delta(n\epsilon) = (1-\Lambda)\Delta p_\Delta(n\epsilon, N\Delta)$$

and hence

$$\frac{\Delta}{\epsilon}\Lambda p_\Delta(n\epsilon, N\Delta) = \frac{\Lambda}{1-\Lambda}\frac{F_\Delta((n+1)\epsilon) - F_\Delta(n\epsilon)}{\epsilon}$$
$$\to \frac{\Lambda}{1-\Lambda}\frac{d}{dt}F(n\epsilon) = -\frac{\Lambda}{1-\Lambda}\int_0^1 \frac{\partial}{\partial t}p(t,x)dx.$$

In this way we get the boundary condition

$$\int_0^1 \lambda(x)p(t,x)dx - \frac{\Lambda}{1-\Lambda}\int_0^1 \frac{\partial}{\partial t}p(t,x)dx + \frac{1}{2}\frac{\partial}{\partial x}(D(x)p(t,x))_{|x=0} - v(0)p(t,0) = 0.$$

The above derivation of the limiting PDE has been largely heuristic. For a rigorous proof we have to view (7) as a numerical solution scheme for the PDE (8) and prove convergence of the numerical solution. In order to minimize notational effort, we will carry this out for the case of constant parameters λ, D, v only. For abbreviation we introduce $p_i^n := p_\Delta(n\epsilon, i\Delta)$, noting that p_i^n implicitly also depends on Δ. Then (7) becomes

$$p_i^{n+1} = \left(\frac{\epsilon}{2\Delta^2}D + \frac{\epsilon}{2\Delta}v\right)(1-\epsilon\lambda)p_{i-1}^n + \left(1 - \frac{\epsilon}{\Delta^2}\right)(1-\epsilon\lambda)p_i^n$$
$$+ \left(\frac{\epsilon}{2\Delta^2}D - \frac{\epsilon}{2\Delta}v\right)(1-\epsilon\lambda)p_{i+1}^n.$$

Subtracting p_i^n from both sides and dividing by ϵ, we get

$$\frac{p_i^{n+1} - p_i^n}{\epsilon} = \frac{D}{2\Delta^2}\left[p_{i+1}^n - 2p_i^n + p_{i+1}^n\right] - \frac{v}{2\Delta}\left[p_{i+1}^n - p_{i-1}^n\right] - \lambda p_i^n$$
$$-\lambda\left[\frac{\epsilon}{2\Delta^2}D\left(p_{i-1}^n - 2p_i^n + p_{i+1}^n\right) - \frac{\epsilon}{2\Delta}v\left(p_{i+1}^n - p_{i-1}^n\right)\right]. \tag{16}$$

Now assume that $\tilde{p}$ is an exact solution to (8) and denote $\tilde{p}(n\epsilon, i\Delta)$ by $\tilde{p}_i^n$. We use a Taylor series expansion of $\tilde{p}$ to get

$$\begin{aligned}
\tilde{p}_i^{n+1} &= \tilde{p}_i^n + \epsilon \left(\frac{\partial \tilde{p}}{\partial t}\right)_i^n + \frac{\epsilon^2}{2}\left(\frac{\partial^2 \tilde{p}}{\partial t^2}\right)_i^{n+\theta_1}, \\
\tilde{p}_{i+1}^n &= \tilde{p}_i^n + \Delta \left(\frac{\partial \tilde{p}}{\partial x}\right)_i^n + \frac{\Delta^2}{2}\left(\frac{\partial^2 \tilde{p}}{\partial x^2}\right)_i^n + \frac{\Delta^3}{6}\left(\frac{\partial^3 \tilde{p}}{\partial x^3}\right)_{i+\theta_2}^n, \\
\tilde{p}_{i-1}^n &= \tilde{p}_i^n - \Delta \left(\frac{\partial \tilde{p}}{\partial x}\right)_i^n + \frac{\Delta^2}{2}\left(\frac{\partial^2 \tilde{p}}{\partial x^2}\right)_i^n - \frac{\Delta^3}{6}\left(\frac{\partial^3 \tilde{p}}{\partial x^3}\right)_{i-\theta_3}^n,
\end{aligned}$$

where $0 \le \theta_1, \theta_2, \theta_3 \le 1$. Following the standard approach (see, e.g., Richtmyer and Morton [16]) we show that $\tilde{p}_i^n$ is an approximate solution to the difference equation (16). Using the above expansions, the difference between the two sides of (16) when p is replaced by $\tilde{p}$ becomes

$$\begin{aligned}
&\frac{\tilde{p}_i^{n+1} - \tilde{p}_i^n}{\epsilon} - \frac{D}{2\Delta^2}\left[\tilde{p}_{i-1}^n - 2\tilde{p}_i^n + \tilde{p}_{n+1}^n\right] + \frac{v}{2\Delta}\left[\tilde{p}_{i+1}^n - \tilde{p}_{i-1}^n\right] + \lambda \tilde{p}_i^n \\
&+\lambda\left\{\frac{\epsilon}{2\Delta^2} D\left[\tilde{p}_{i-1}^n - 2\tilde{p}_i^n + \tilde{p}_{i+1}^n\right] - \frac{\epsilon}{2\Delta} v\left[\tilde{p}_{i+1}^n - \tilde{p}_{i-1}^n\right]\right\} \\
&= \left(\frac{\partial \tilde{p}}{\partial t}\right)_i^n + \frac{\epsilon}{2}\left(\frac{\partial^2 \tilde{p}}{\partial t^2}\right)_i^{n+\theta_1} \\
&-\frac{D}{2\Delta^2}\left[\Delta^2\left(\frac{\partial^2 \tilde{p}}{\partial x^2}\right)_i^n + \frac{\Delta^3}{6}\left(\frac{\partial^3 \tilde{p}}{\partial x^3}\right)_{i+\theta_2} - \frac{\Delta^3}{6}\left(\frac{\partial^3 \tilde{p}}{\partial x^3}\right)_{i-\theta_3}\right] \\
&+\frac{v}{2\Delta}\left[2\Delta\left(\frac{\partial \tilde{p}}{\partial x}\right)_i^n - \frac{\Delta^3}{6}\left(\frac{\partial^3 \tilde{p}}{\partial x^3}\right)_{i+\theta_2}^n + \frac{\Delta^3}{6}\left(\frac{\partial^3 \tilde{p}}{\partial x^3}\right)_{i-\theta_3}^n\right] + \lambda \tilde{p}_i^n \\
&+\lambda\left\{\frac{\epsilon}{2\Delta^2} D\left[\Delta^2\left(\frac{\partial^2 \tilde{p}}{\partial x^2}\right)_i^n + \frac{\Delta^3}{6}\left(\frac{\partial^3 \tilde{p}}{\partial x^3}\right)_{i+\theta_2} - \frac{\Delta^3}{6}\left(\frac{\partial^3 \tilde{p}}{\partial x^3}\right)_{i-\theta_3}\right]\right. \\
&\left.-\frac{\epsilon}{2\Delta} v\left[2\Delta\left(\frac{\partial \tilde{p}}{\partial x}\right)_i^n - \frac{\Delta^3}{6}\left(\frac{\partial^3 \tilde{p}}{\partial x^3}\right)_{i+\theta_2}^n + \frac{\Delta^3}{6}\left(\frac{\partial^3 \tilde{p}}{\partial x^3}\right)_{i-\theta_3}^n\right]\right\} \\
&= \left(\frac{\partial \tilde{p}}{\partial t}\right)_i^n - \frac{D}{2}\left(\frac{\partial^2 \tilde{p}}{\partial x^2}\right)_i^n + v\left(\frac{\partial \tilde{p}}{\partial x}\right)_i^n + \lambda \tilde{p}_i^n + O(\epsilon + \Delta) \\
&= O(\epsilon + \Delta),
\end{aligned}$$

where the last equality holds since $\tilde{p}$ solves the PDE (8).

We then define $r := \tilde{p} - p$. Combining the difference equations for p and $\tilde{p}$, we obtain for r

$$\begin{aligned}
\frac{r_i^{n+1} - r_i^n}{\epsilon} = &\frac{D}{2\Delta^2}\left[r_{i-1}^n - 2r_i^n + r_{i+1}^n\right] - \frac{v}{2\Delta}\left[r_{i+1}^n - r_{i-1}^n\right] - \lambda r_i^n \\
&-\lambda\left[\frac{\epsilon}{2\Delta^2}\left(r_{i-1}^n - 2r_i^n + r_{i+1}^n\right) - \frac{\epsilon}{2\Delta} v\left(r_{i+1}^n - r_{i-1}^n\right)\right] \\
&+O(\epsilon + \Delta).
\end{aligned}$$

This yields the following recursion equation for r_i^{n+1}:

$$r_i^{n+1} = r_i^n + \frac{\epsilon\Delta}{2\Delta^2}\left[r_{i-1}^n - 2r_i^n + r_{i+1}^n\right] - \frac{\epsilon v}{2\Delta}\left[r_{i+1}^n - r_{i-1}^n\right] - \epsilon\lambda r_i^n$$

$$
\begin{aligned}
&-\frac{\lambda\epsilon^2 D}{2\Delta^2}\left[r_{i-1}^n - 2r_i^n + r_{i+1}^n\right] + \frac{\lambda\epsilon^2 v}{2\Delta}\left[r_{i+1}^n - r_{i-1}^n\right] + \epsilon O(\epsilon+\Delta)\\
&= r_{i-1}^n\left[\frac{\epsilon D}{2\Delta^2} + \frac{\epsilon v}{2\Delta} - \frac{\lambda\epsilon^2 D}{2\Delta^2} - \frac{\lambda\epsilon^2 v}{2\Delta}\right]\\
&\quad + r_i^n\left[1 - \frac{\epsilon D}{\Delta^2} - \epsilon\lambda + \frac{\lambda\epsilon^2 D}{\Delta^2}\right]\\
&\quad + r_{i+1}^n\left[\frac{\epsilon D}{2\Delta^2} - \frac{\epsilon v}{2\Delta} - \frac{\lambda\epsilon^2 D}{2\Delta^2} + \frac{\lambda\epsilon^2 v}{2\Delta}\right] + \epsilon O(\epsilon+\Delta).
\end{aligned}
$$

The sum of the coefficients in the brackets on the right-hand side equals $1-\epsilon\lambda$. Under the stability condition $\frac{\epsilon D}{\Delta^2} < 1$, all coefficients eventually become ≥ 0, and thus we may conclude that

$$\max_i |r_i^{n+1}| \leq \max_i |r_i^n| + \epsilon O(\epsilon+\Delta).$$

Iterating this inequality and using the fact that $r_i^0 \equiv 0$, we find

$$\max_i |r_i^{n+1}| = n\epsilon O(\epsilon+\Delta) = tO(\epsilon+\Delta),$$

implying convergence of $\tilde{p} - p$ to 0 as $\epsilon, \Delta \to 0$.

Note added in proof. Convergence of the discrete stochastic process $(X_t^\delta)_t \geq 0$ to a limit process $(X_t)_t \geq 0$ has, in the meantime, been established rigorously by Dabowski and Dehling [3]. They showed that the limit process can be represented as a diffusion process with trajectory dependent jump rate.

Acknowledgments. The authors would like to thank the referees of this paper for their careful reading of the manuscript and for their thoughtful comments, which greatly helped to improve the presentation.

REFERENCES

[1] F. Berruti, A.G. Liden, and D.S. Scott, *Measuring and modelling residence time distribution of low density solids in a fluidized bed reactor of sand particles*, Chem. Engrg. Sci., 43 (1988), pp. 739–748.

[2] R.N. Bhattacharya and E.C. Waymire, *Stochastic Processes with Applications*, John Wiley, New York, 1990.

[3] A.R. Dabrowski and H.G. Dehling, *Jump diffusion approximation for a Markovian transport model*, in Asymptotic Mathods in Probability and Statistics, B. Szyszkowicz, ed., Elsevier Science, North–Holland, Amsterdam, 1998, pp. 115–125.

[4] D. Geldart, *The effect of particle size and size distribution on the behaviour of gas-fluidized beds*, Powder Tech., 6 (1972), pp. 201–215.

[5] A.K. Haines, R.P. King, and E.T. Woodburn, *The interrelationship between bubble motion and solids mixing in a gas fluidized bed*, AIChE J., 18 (1972), pp. 591–599.

[6] G.J. Hartholt, *Particle mixing in gas fluidized beds*, Ph.D. thesis, Department of Chemical Engineering, University of Groningen, Groningen, The Netherlands, 1996.

[7] P.M. Heertjes, L.H. de Nie, and J. Verloop, *Transport and residence time of particles in a shallow fluidized bed*, in Proceedings of the International Symposium on Fluidization, A.A.H. Drinkenburg, ed., Eindhoven, The Netherlands, Netherlands University Press, Amsterdam, 1967.

[8] A.C. Hoffmann and H. Paarhuis, *A study of the particle residence time distribution in continuous fluidized beds*, I. Chem. E. Sympos. Ser., 121 (1990), pp. 37–49.

[9] A.C. Hoffmann, L.P.B.M. Janssen, and J. Prince, *Particle segregation in fluidized binary mixtures*, Chem. Engrg. Sci., 48 (1993), pp. 1583–1592.

[10] E. Klose and W. Heschel, (1985). *Zur Messung der Partikelverweilzeitverteilung in Wirbelschichten mit Gas-Feststoff-Reaktion*, Chem. Techn., 37 (1985), pp. 149–152.

[11] K. Krishnaiah, Y. Pydisetty, and Y.B.G. Varma, *Residence time distribution of solids in multistage fluidization*, Chem. Engrg. Sci., 37 (1982), pp. 1371–1377.
[12] R. la Riviére, G.P. Hartholt, A.C. Hoffmann, and L.P.B.M. Janssen, *Methods for the determination of particle residence time distribution in continuous gas fluidized beds*, I. Chem. E. Sympos. Ser., 140 (1996), pp. 283–294.
[13] L. Massimilla and S. Bracale, *Il mescolamento della fase solida nei sistemi: Solido-gas fluidizzati, liberi e frenati*, La Ricerca Scientifica, 27 (1957), pp. 1509–1526.
[14] D.R. Morris, K.E. Gubbins, and Watkins, *Residence time studies in fluidized and moving beds with continuous solids flow*, Trans. Inst. Chem. Engrs., 42 (1964), pp. T323–T333.
[15] F. Pudel, M. Strümke, and U. Sündermann, *Untersuchung des Partikelverweilzeitverhaltens in Gas-Feststoff-Wirbelrinnen*, Wiss. Z. Tech. Hochsch. Magdeburg, 30 (1986), pp. 51–53.
[16] R.D. Richtmyer and K.W. Morton, *Difference Methods for Initial-Value Problems*, John Wiley, New York, 1967.
[17] P.N. Rowe and B.A. Partridge, *Particle movement caused by bubbles in a fluidized bed*, in Interaction Between Fluids & Particles, Inst. Chem. Engrs., London, 1962, pp. 135–142.
[18] G. Tripathi, G.N. Pandey, and P.C. Singh, *Residence time distribution studies on different systems: Derivation of a generalized correlation*, Indian J. Tech., 9 (1971), pp. 281–284.
[19] J. Verloop, L.H. De Nie, and P.M. Heertjes, *The residence time of solids in gas-fluidized beds*, Powder Tech., 2 (1968/69), pp. 32–42.
[20] B. Weber and K. Rose, *Mathematische Modelliering von Wirbelschichten*, Chem. Techn., 22 (1970), pp. 594-596.
[21] J. Werther, *Influence of the bed diameter on the hydrodynamics of gas fluidized beds*, AIChE Sympos. Ser., 70 (1974), pp. 53–62.
[22] K. Whittmann, D. Wippern, H. Schlingmann, H. Helmrich, and K. Schügerl, *Solid particle mixing in a continuously operated fluidized bed reactor*, Chem. Engrg. Sci., 38 (1983), pp. 1391–1397.